AD-A099 180 CALIFORNIA UNIV DAVIS DEPT OF APPLIED SCIENCE F/G 20/12
EXPERIMENTAL AND THEORETICAL STUDY OF THE FEASIBILITY OF THE GU--ETC(U)
MAR 81 C FONG, F WOOTEN AFOSR-77-3390

UNCLASSIFIED AFOSR-TR-81-0452 NL

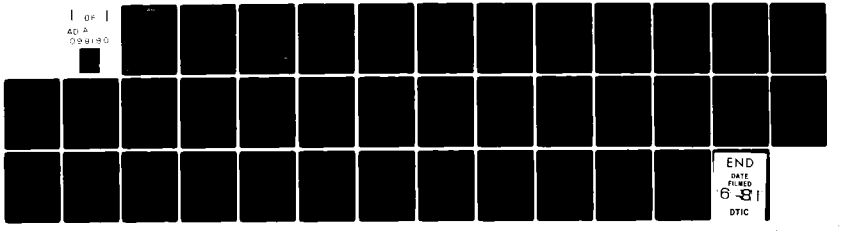

UNCLASSIFIED

SECURITY CLASSIFICATION OF THIS PAGE (When Data Entered)

LEVEL II

REPORT DOCUMENTATION PAGE

READ INSTRUCTIONS BEFORE COMPLETING FORM

1. REPORT NUMBER AFOSR-TR- 81 0452	2. GOVT ACCESSION NO. AD-A099180
	3. RECIPIENT'S CATALOG NUMBER
EXPERIMENTAL AND THEORETICAL STUDY OF THE FEASIBILITY OF THE GUNN EFFECT IN BiSCl, BiSBr, BiSI, BiSeI, BiSeBr, and BiSeCl	5. TYPE OF REPORT & PERIOD COVERED Final
	6. PERFORMING ORG. REPORT NUMBER
7. AUTHOR(s) C. Y. Fong and F. Wooten	8. CONTRACT OR GRANT NUMBER(s) AFOSR-77-3390
9. PERFORMING ORGANIZATION NAME AND ADDRESS Department of Applied Science University of California Davis, CA 95616	10. PROGRAM ELEMENT, PROJECT, TASK AREA & WORK UNIT NUMBERS 2306/B2 61102F
11. CONTROLLING OFFICE NAME AND ADDRESS Air Force Office of Scientific Research Bolling AFB, Bldg. 410 Washington, D.C. 20332	12. REPORT DATE March 1981 13. NUMBER OF PAGES 35
14. MONITORING AGENCY NAME & ADDRESS(if different from Controlling Office)	15. SECURITY CLASS. (of this report) Unclassified 15a. DECLASSIFICATION/DOWNGRADING SCHEDULE

16. DISTRIBUTION STATEMENT (of this Report)

Approved for public release;
distribution unlimited.

17. DISTRIBUTION STATEMENT (of the abstract entered in Block 20, if different from Report)

DTIC ELECTE MAY 20 1981 E

18. SUPPLEMENTARY NOTES

19. KEY WORDS (Continue on reverse side if necessary and identify by block number)

20. ABSTRACT (Continue on reverse side if necessary and identify by block number)

The optical reflectance of BiSI has been measured with photon energy, from 1.2 to 3.6 eV. The band structures of BiSBr, BiSCl, BiSeBr, BiSeCl and BiSeI have been calculated by using the self-consistent pseudopotential method. These results show that: (i) they are indirect gap semiconductors; (ii) the top of the valence band is located at some k-point along rZ (the z-direction) with finite curvature (small effective mass); (iii) the highest valence band at r (the center of the Brillouin zone) is only a few tenths of an eV lower than the energy of the top of the valence band and is flat (large effective mass).

DD FORM 1 JAN 73 1473 EDITION OF 1 NOV 65 IS OBSOLETE

Unclassified
SECURITY CLASSIFICATION OF THIS PAGE (When Data Entered)

AD A099180

DTIC FILE COPY

especially in the directions perpendicular to z. (iv) in addition to the above listed features, the minimum of the conduction band for BiSCl and BiSeCl is located at some k-point along rX, the x direction and is a few tenths of an eV lower than the lowest conduction band at r.

These results suggest that: All the six compounds studied in this project will exhibit the Gunn effect if they are properly doped. They are potential candidates for microwave oscillators.

EXPERIMENTAL AND THEORETICAL STUDY OF THE FEASIBILITY OF THE GUNN EFFECT IN BiSCl, BiSBr, BiSI, BiSeI, BiSeBr AND BiSeCl*

Final Scientific Report

by

C. Y. Fong and F. Wooten

Department of Applied Science
University of California
Davis, CA 95616

*Supported by US Air Force Office of Scientific Research under Grant No. AFOSR-77-3390

ABSTRACT

The optical reflectance of BiSI has been measured with photon energy, $\hbar\omega$, from 2.2 to 3.6 eV. The band structures of BiSBr, BiSCl, BiSI, BiSeBr, BiSeCl and BiSeI have been calculated by using the self-consistent pseudopotential method. These results show that: (i) they are indirect gap semiconductors; (ii) the top of the valence band is located at some $\vec{k}$-point along ΓZ (the $\hat{z}$-direction) with finite curvature (small effective mass); (iii) the highest valence band at Γ (the center of the Brillouin zone) is only a few tenths of an eV lower than the evergy of the top of the valence band and is flat (large effective mass), especially in the directions perpendicular to $\hat{z}$. (iv) in addition to the above listed features, the minimum of the conduction band for BiSCl and BiSeCl is located at some $\vec{k}$-point along ΓX, the $\hat{x}$-direction and is a few tenths of an eV lower than the lowest conduction band at Γ.

These results suggest that: All the six compounds studied in this project will exhibit the Gunn effect if they are properly doped. They are potential candidates for microwave oscillators.

The dopings in BiSBr, BiSeBr, BiSI and BiSeI should be restricted to p-type. Effective doping to exhibit the Gunn effect will be to substitute either the group IV elements for Bi or the group V elements for Se. For BiSCl and BiSeCl, both n and p-type dopings are possible. The p-type doping should be restricted to the same elements as suggested for the other four crystals. The best results for n-type doping should be obtained by substituting the Bi by the group VI elements.

The electric field used for the Gunn effect should be applied along the $\hat{z}$-direction for the p-type dopings. It is necessary to apply the electric field in the $\hat{x}$-direction in order to exhibit the Gunn effect in n-type crystals.

Comparisons of the other available experimental gap energies with the theoretical results are made. Discrepancy between the measured and calculated trend of gap values in I- and Br- compounds is discussed and a possible explanation is provided.

The bonding properties of these crystals are presented.

I. INTRODUCTION

The objective of this grant (No. 77-3390) is to show whether BiSBr, BiSCl, BiSI, BiSeBr, BiSeCl and BiSeI are candidates for microwave oscillators.

The criterion for a crystal to be used as a microwave oscillator is that it should exhibit the Gunn effect. Consider a degenerate n-doped semiconductor, then there are electrons in the conduction band even at T = 0°K. The current density under the influence of an externally applied dc field is given by

$$\bar{J} = \sigma\bar{\varepsilon} \qquad (1)$$

where $\bar{\varepsilon}$ is the electric field, and σ is the conductivity. Let ρ and τ be the density and the life time of the electrons, then

$$\sigma = \frac{\rho e^2 \tau}{m^*} \qquad (2)$$

where m* is the effective mass of the electrons. From the analogy of the free electron case $\frac{1}{m} = \frac{1}{\hbar^2}\frac{\partial^2 E}{\partial k^2}$, the value of m* is inversely proportional to the curvature of the energy with respect to the crystal momentum of an electron.

As the electric field is increased, not only does it accelerate the electrons but also it causes scattering of the electrons. The scattered electrons can be in states such that their effective masses increase. Consequently σ decreases and so does the current. The typical J vs ε curve is shown in Fig. 1. The region A indicates that current decreases as the strength of the applied field increases. The sample exhibits a negative conductivity. This is the Gunn effect.

If one recognizes that positive σ represents power consumption, it is clear that negative σ means that the sample supplies power, and can be used as an oscillator.

From the above discussions, it is apparent that we need to find the band structure, $E(\bar{k})$, for the electrons in a semiconductor, then decide whether it can be used as an oscillator. We believe that this is the first study of this kind for the Bi-compounds.

In Section II, we discuss the experimental set up for the reflectance measurements. The method used for calculating the band structure will be described in Section III. The results and the discussions about the basic properties and applications will be presented in Section IV. Finally, in Section V concluding remarks will be given.

II. EXPERIMENTAL ASPECT

Reflectance data were obtained for samples of the crystals BiSI. Originally, the crystal samples were in a matted form with small quantities of reactant materials filling the interstitial space between the actual crystals of the material of interest. The samples were washed with a 56% solution of HI, then methanol, then acetone several times each. The cleaned crystal samples were then mounted on an aluminum sample holder and placed in the reflectance chamber.

The range of the scans was from 3350 Å to 5400 Å. The light source used was a tungsten filament lamp. The light detector was an uncoated photomultiplier tube (number 9843B from EMI GENCOM) with an S-11 response, operated between 800 and 1000 volts. The tube was electrostatically and magnetically shielded and all the electronics shared a common ground to reduce noise as much as possible. A signal to noise ratio of 25 was typical. Typical dark count was 0.2 microamps. A more complete description of the reflectance chamber and the optical system has been presented elsewhere.[1] A schematic diagram is shown in Fig. 2.

The measurements were performed at atmospheric pressure since absorption in the visible range is not a problem, and no filter was used for the final runs as there was no discernible difference either way.

The reflectance data are the relative reflectance of the samples. The ellipsoidal mirror assembly was adjusted to occult the reference beam in such a way as to obtain optimal reflectances. If the full intensity of the reference beam were used, the reflected signal would be relatively too weak, producing a small and noisy relative reflectance curve. The mirror position was adjusted for each sample to maximize the relative reflectance and to minimize noise.

To perform a data scan, the monochromator was set at 3350 Å, the increment (5Å) and the number of data points (410) were entered into the reflectance program, which carried out the scan automatically. The data were then plotted as a graph of relative reflectance versus energy or wavelength.

III. METHOD OF CALCULATIONS

The self-consistent pseudopotential method is used to calculate the band structures of the 6 Bi-compounds. The procedures involved in the method are summarized schematically in the block diagram (Fig. 3).

The ionic pseudopotentials of Bi, Se, I, Br were determined by the local scheme proposed by Starkloff and Joannopoulos.[2] The essential feature of the scheme is to multiply the self-consistent atomic potential[3] by a function which has the following form

$$f = \frac{1 - e^{-\lambda r}}{1 + e^{-\lambda(r-r_c)}} \qquad (3)$$

This function weakens the potential for $r<r_c$ and approach 1 for $r>r_c$. The λ and r_c are determined by fitting the valence state energies to the atomic calculations.[3] Thus, the resulting ionic pseudopotential (effective potential) gives the same atomic energies as in the full self-consistent calculations.

For S and Cl, the extrema of the outermost s and p states are very close together ($\sim$0.1 Å) as given in Ref. 3. It is difficult to use the f-function, Eq. (3), to fit simultaneously the s and p states energies. By making use of the non-uniqueness of the pseudopotential in the core region, we added a repulsive s-potential of Gaussian form in the core region. The Gaussian potential has the form:

$$V_s(r) = Ar^2 e^{-\alpha r^2} \qquad (4)$$

The charge densities used for the initial construction of the electron-electron interaction -- Coulomb and exchange potentials -- were obtained from earlier empirical pseudopotential calculations of the Sb-compounds.[4] We used the so called $X\alpha$ - exchange of Slater[5], and set $\alpha = 1$.

The self-consistent cycles were carried out at one special $\bar{k}$ point (0.25a; 0.25b, 0.117c) where b is the longest and c is the shortest lattice constant. The charge densities associated with this $\bar{k}$ point do not overlap with the ones of 4 nearest unit cells[6].

To assure the convergence of the energy eigenvalue with respect to the number of plane waves, we used about 380 planes waves as basis functions. In addition, there are another 380 plane waves included via the Löwdin perturbation[7].

It took about 8 cycles in each crystal for the potential to attain self-consistency. The resulting electron-electron interaction and the ionic pseudopotentials are used to calculate the band structure, E vs $\bar{k}$.

IV. RESULTS AND DISCUSSION

The measured reflectance of BiSI for photon energy, $\hbar\omega$, between 2.2 to 3.5 eV is shown in Fig. 4. The structures at 2.3 and 2.6 eV in the present results correspond to the double structure of 2.2 and 2.4 eV in SbSI. Tentative identification of the origins of the two structures will be presented later.

Let's turn our attention to the results of the self-consistant calculations. It is necessary to show how good the ionic pseudopotentials are. We choose I as an example to show the comparison of the ionic pseudopotential and the full self-consistent (core included) ionic potential.[3] The two potentials are compared in Fig. 5a. For $r > 3$.a.u., perfect agreement of the two potentials is obtained. The pseudopotential in the region $r < 3$, is considerably weaker than V_{ionic}. The pseudo wavefunctions of the s and the p states are compared with the full self-consistent results in Fig. 5b. Outside r_c, the pseudo wavefunctions agree reasonably with those of the full self-consistent calculations. In the core region, the pseudo wavefunctions are smoother, i.e. no wiggling, than the exact wavefunctions. The ionic pseudopotentials of other elements show similar features. So, we simply plotted the pseudopotentials of Bi, S, Se, Br and Cl, in Fig. 6a-6e. The values of r_c and λ for Bi, Se, Br, I are listed in Table I along with the comparisons of the fitted valence states energies and those given by full self-consistent calculations using the Herman-Skillman programs. Parameters characterizing potentials for S and Cl are given in Table II. These potentials will also be useful for future calculations of semiconducting solids with these elements as constituents. The Se results have been checked with the ones determined by Joannopoulos.[8]

The band structures of the six compounds are plotted along the crystal axes in Fig. 7a-7f. Since our present interests are those bands near the fundamental gap, only 6 bands below and 4 bands above the gap are given.

There are several common features in these calculations. They are:

(i) All of these crystals are indirect gap semiconductors.

(ii) The top of the valence band is located at some $\bar{k}$-point, $\bar{k}_0$, along ΓZ (z-direction) and is a few tenths of an eV above the highest valence band energy at Γ ($\bar{k}=0$).

(iii The valence band along the $\hat{a}$ ($\hat{x}$) and $\hat{b}$ ($\hat{y}$) directions have less dispersion (curvature) than the ones along the $\hat{c}$ ($\hat{z}$) axis.

Feature (i) agrees qualitatively with our earlier empirical calculations of Sb-compounds.[4] Most of the Sb-compounds, however, have the top of the valence bands at Γ. The joint features of (i) and (ii) indicate that the curvature of the top of the valence band is greater than that at Γ. Consequently, the effective mass of the hole at Γ is larger than that at the valence band edge. Coupled with the small energy difference at $\bar{k}_0$ and Γ, these crystals should exhibit the Gunn effect if they are p-dopped (e.g. S or Se to be replaced by P, or As). Therefore, we find that these six crystals are potential candidates for microwave oscillators. Finally, the third feature, the difference in dispersion along the different axes, is a manifestation of the anisotropy in the crystal structure of these compounds.

The characteristics of the conduction bands show more variation for the 6 crystals than those exhibited in the valence bands. The Br and I-compounds have the minimum of the conduction bands at Γ, while the two Cl-semiconductors exhibit the minimum at some $\bar{k}$-point along ΓX ($\hat{x}$-direction). Therefore, the Br and I crystals have the smallest direct gap at Γ and the gap for both BiSCl and BiSeCl appears along ΓX. The values of the lattice constants, the fundamental gaps and the smallest direct gaps for these Bi-compounds are summarized in Table III accompanied by a few measured gap values.

The difference in the conduction bands of the Cl-crystals from the ones of the other compounds makes the possibility of exhibiting the Gunn effect in n-type BiSCl and BiSeCl. In these cases, the electric field should be applied along the $\hat{x}$-direction.

From Table III, one notices that BiSCl and BiSeCl have the same lattice constants. This deserves some explanation. We are unable to find the lattice constants of BiSeCl in the literature. As a first trial, the lattice constants of BiSeI were used. The self-consistent calculations show that BiSeCl is a semimetal. Next, we tried the lattice constants of BiSeBr. A similar result was obtained. This suggests BiSeCl may be a semimetal. However, we reject this possibility based on the calculated total valence bandwidth. Both results show that the width is about 24 eV, which is roughly a factor of 2 wider than the other five compounds. There does not exist any plausible physical mechanism to cause the large width in the BiSeCl except that the lattice constants used for the calculations are too large. Finally, we used the lattice constants of BiSCl. Results seem in line with the others. However, as seen in Table III, it has still the smallest fundamental gap. One would expect that the lattice constants of BiSeCl should be larger than the ones of BiSCl based simply on the sizes of Se and S. The difficulty in obtaining a reasonable band structure of BiSeCl suggests that the crystal may not be stable under normal conditions (atmospheric pressure). Our calculations correlate the absence of crystallographic data for this particular crystal.

Another point given in Table III is worth explanation. We see that the calculated band gaps of BiSeI and BiSeBr are comparable. Because the same experimental group has reported two different gap values of BiSeI at different times, it is difficult to argue that either of the experimental values are more accurate than the theoretical prediction. We, then, turn our attention to examine the charge density of these two crystals. Intuitively, one would say that since Br is more electronegative than I, BiSeBr should have a larger gap than BiSeI. However, we found that this is too simple a picture. In Fig. 8a-8b we compare the total valence charge densities of these two crystals in a section consisting of Bi, Se, and a halide. The atoms are labeled in the figures. Comparing the charge densities around the halides, we see that the Br has more charge than the I. This result is consistent with the intuitive feeling. Now, let us look at the charge density between the Bi-Se bonds. The I-crystal has more bond charge than the other. We can conclude that BiSeBr is more ionic between the Bi-Br bond but less covalent in the Bi-Se bond, whereas BiSeI is just the reverse. How does this bonding property influence the value of the energy gap? We examine the charge densities from the four highest valence bands. In order to show more clearly the features, we choose a section (II in Fig. 9) consisting of the same Bi and halides but the Se forming the horizontal bond with the Bi. In Fig. 10a and 10b, the valence charge densities of BiSeBr and BiSeI in Section II are plotted. Both BiSeBr and BiSeI exhibit more charge around the Bi and Se than around the halides. So, the ionic character of the I and Br should be manifested by the charges associated with lower energy valence states. Because of the stronger ionic nature of the Br, the bond between the Bi and the Se is less covalent. As a result, the BiSeBr has a smaller gap than BiSeI. Furthermore, from the charge densities shown in Fig. 10, we suggest that the p-doping of these crystals will not be effective for exhibiting the Gunn effect, if the halides are substituted by group VI elements. It is necessary to substitute either the Bi by group IV elements or the chalcogenides by group V elements. For n-doping, only substitution of Bi by group VI elements will be effective. The charge of the lowest conduction band should be associated with the Bi-atom, because as shown in Figs. 11a, b the corresponding charge distributions are around the metal ion.

Using the band structure of BiSI, and the earlier interpretation of the Sb-compounds, the structures at 2.4 and 2.6 eV in the reflectance are inferred to be mainly caused by the transitions from states near Γ_8 to states near Γ_6 along ΓZ.

IV. CONCLUSION

We have measured the reflectance of BiSI and calculated the band structure of the six Bi-compounds. The self-consistent pseudopotential method is used for the calculations. The results show:

A. All the six Bi-compounds are potential candidates for microwave oscillators, if (a) all of them are p-dopped; (b) the BiSCl and the BiSeCl are n-dopped; (c) BiSeCl cannot be grown under atmospheric pressure.

B. Smaller lattice constants are necessary for the semiconducting behavior of BiSeCl. Apparently, there does not exist any crystallographic data of BiSeCl. This is consistent with the difficulty in getting reasonable band structure.

C. The doping should be specific in these crystals. For p-doping, substituting either the group IV elements for Bi or the group V elements for the chalcogenides is the effective way. The Gunn effect is not expected to be observed if one substitutes for the halides. For n-type doping, the only substitution to exhibit the Gunn effect is to replace the Bi by the group VI elements.

D. For p-type doping, the d.c. field is to be applied along the $\hat{z}$-direction, i.e. the direction of the needle. For n-type doping, the d.c. field should be applied along the $\hat{x}$-direction.

In addition to the above findings for the microwave oscillators, we also cite the following basic properties:

E. These six compounds are indirect semiconductors.

F. The bands along the $\hat{z}$-direction are in general more dispersive than those along the $\hat{x}$ and the $\hat{y}$-directions.

G. There are two different types of bonding in these crystals. Ionic bonding appears between Bi and the halides. These ionic states form the lower energy valence bands. The bonding between the Bi and the chalcogenides is substantially of covalent character. The states associated with this bonding contribute to the bands near the fundamental gap.

H. The value of the fundamental gap is determined by the interplay of the ionic and the covalent bondings. More ionic bonding means less charge is available to form the covalent bonding. Consequently, the value of the gap is smaller.

References

1. T. Huen, G. B. Irani and F. Wooten, Applied Optics 10, 552 (1971).
2. Th. Starkloff and J. D. Joannopoulos, Phys. Rev. B 19, 1077 (1979).
3. F. Herman and S. Skillman, Atomic Structure Calculations, Prentice Hall, New Jersey, 1963.
4. J. Alward, C. Y. Fong, M. El-Batanouny and F. Wooten, Solid State Comm. 25, 307 (1978).
5. J. C. Slater, Quantum Theory of Molecules and Solids, Vol. 4, p. 35, McGraw-Hill, New York, 1974.
6. J. D. Joannopoulos and M. L. Cohen, J. Phys. C: Solid St. Phys. 6, 1572 (1973).
7. For examples, D. Brust, Phys. Rev. 134A, 1337 (1964).
8. J. D. Joannopoulos, private communication.
9. D. V. Chepur, D. M. Bercha, I. D. Turyaritsa and V. Yu Slivka, Phys. Status Solids, 30, 461 (1968).
10. O. V. Luksha, A. P. Zhdankin, L. M. Suslikov, N. I. Davogsher and V. Yu Slivka, Soviet Phys. J. 18, 724 (1975).

Table Captions

Table I. The values of λ and r_c for Bi, Se, Br, I and the comparison of the fitted and the reference atomic energies.

Table II. The parameters to characterize the ionic pseudopotentials of Cl and S.

Table III. The lattice constants, the values of the fundamental gaps, the smallest direct gaps and the available experimental gap values.

Figure Captions

Fig. 1. Typical J vs. ε curve for the Gunn effect.

Fig. 2. Schematic diagram of system for reflectance measurements.

Fig. 3. The block diagram of the self-consistent pseudopotential method.

Fig. 4. Reflectance of BiSI.

Fig. 5a. Comparison of the ionic pseudopotential and full self-consistent potential of I.

5b. Comparison of the pseudo wavefunctions and the full self-consistent (exact) wavefunctions of the s and p states of I.

Fig. 6a. Ionic pseudopotentials of Bi.

6b. Ionic pseudopotential of S.

6c. Ionic pseudopotential of Se.

6d. Ionic pseudopotential of Br.

6e. Ionic pseudopotential of Cl.

Fig. 7a. The band structure of BiSBr

7b. The band structure of BiSeBr

7c. The band structure of BiSCl

7d. The band structure of BiSeCl

7e. The band structure of BiSI

7f. The band structure of BiSeI

Fig. 8a. The total valence charge densities of BiSeBr.

8b. The total valence charge densities of BiSeI.

Fig. 9. Atomic configuration in a unit cell.

Fig. 10a. The charge densities of 4 highest valence bands of BiSeBr.

10b. The charge densities of 4 highest valence bands of BiSeI.

Fig. 11a. The charge densities of the lowest conduction band of BiSeBr.

11b. The charge densities of the lowest conduction band of BiSeI.

Table I

	$\lambda(1/a_o)$*	$r_c(a_o)$	Energy of the s state (ryd.)		Energy of the p state (ryd.)	
			H-S Value	Present Result	H-S Value	Present Result
Bi	3.737	1.299	-1.042	-1.042	-0.513	-0.513
I	4.985	1.0697	-1.4296	-1.4292	-0.7341	-0.7345
Se	8.8779	0.9051	-1.495	-1.496	-0.701	-0.701
Br	8.6665	0.899	-1.7185	-1.718	-0.8247	-0.824

* a_o = Bohr radius

Table II

	$\alpha(\mathring{A}^{-2})$	$A(ryd/\mathring{A}^{2})$	$r_c(A_o)$	$\lambda(1/a_o)$	s-state energy (ryd.)		p-state energy (ryd.)	
					Present Result	H-S	Present Result	H-S
Cl	0.857	2.938	0.58	9.2033	-1.812	-1.812	-0.909	-0.907
S	0.961	1.975	0.71	9.2533	-1.531	-1.530	-0.755	0.756

Table III

Crystal	a(Å)	b(Å)	c(Å)	Calculated Indirect Gap (eV)	Calculated Direct Gap (eV)	Measured energy gap (eV) E_I	Measured energy gap (eV) E_{II}
BiSCl	7.7	9.87	4.0	0.74	1.1	1.93[9]	1.89[9]
BiSBr	8.02	9.70	4.01	1.39	1.55	1.97[9]	1.95[9]
BiSI	8.46	10.15	4.14	1.5	1.65	1.58[9]	1.56[9]
BiSeI	8.71	10.54	4.19	0.8	1.15	1.32[9] (0.75[10])	1.3[9]
BiSeBr	8.18	10.47	4.11	0.87	0.97	1.54[9]	1.5[9]
BiSeCl	7.7	9.87	4.0	0.27	0.45		

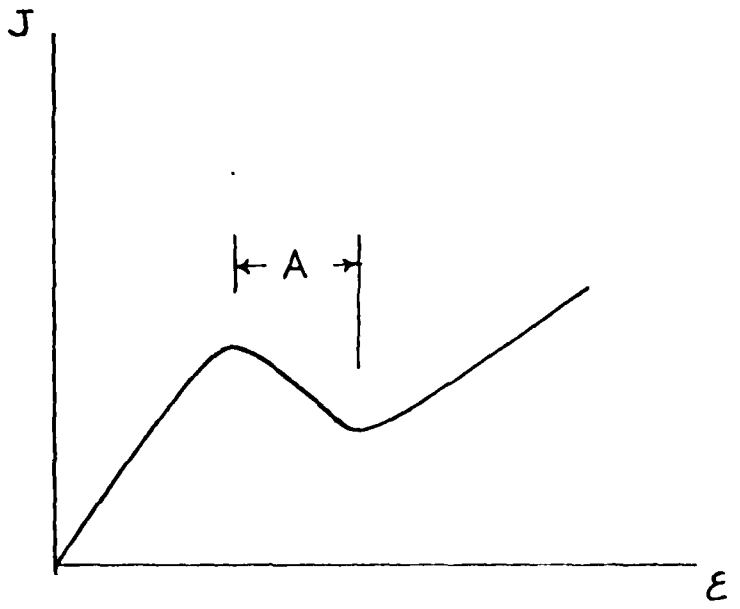

Figure 1

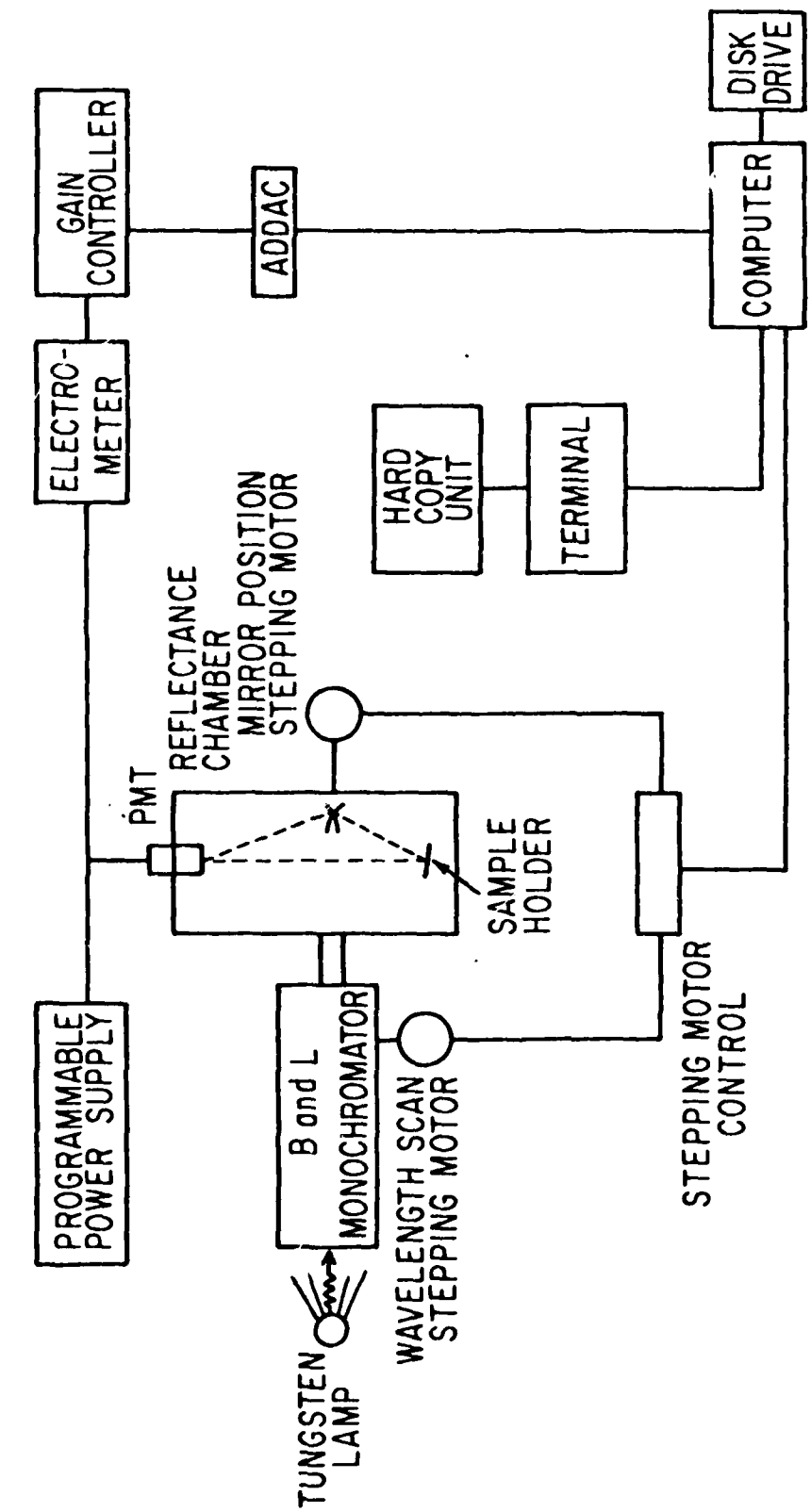
PROGRAMMABLE POWER SUPPLY
ELECTRO-METER
GAIN CONTROLLER
ADDAC
COMPUTER
DISK DRIVE
HARD COPY UNIT
TERMINAL
REFLECTANCE CHAMBER
MIRROR POSITION STEPPING MOTOR
PMT
SAMPLE HOLDER
B and L MONOCHROMATOR
WAVELENGTH SCAN STEPPING MOTOR
STEPPING MOTOR CONTROL
TUNGSTEN LAMP

Figure 2

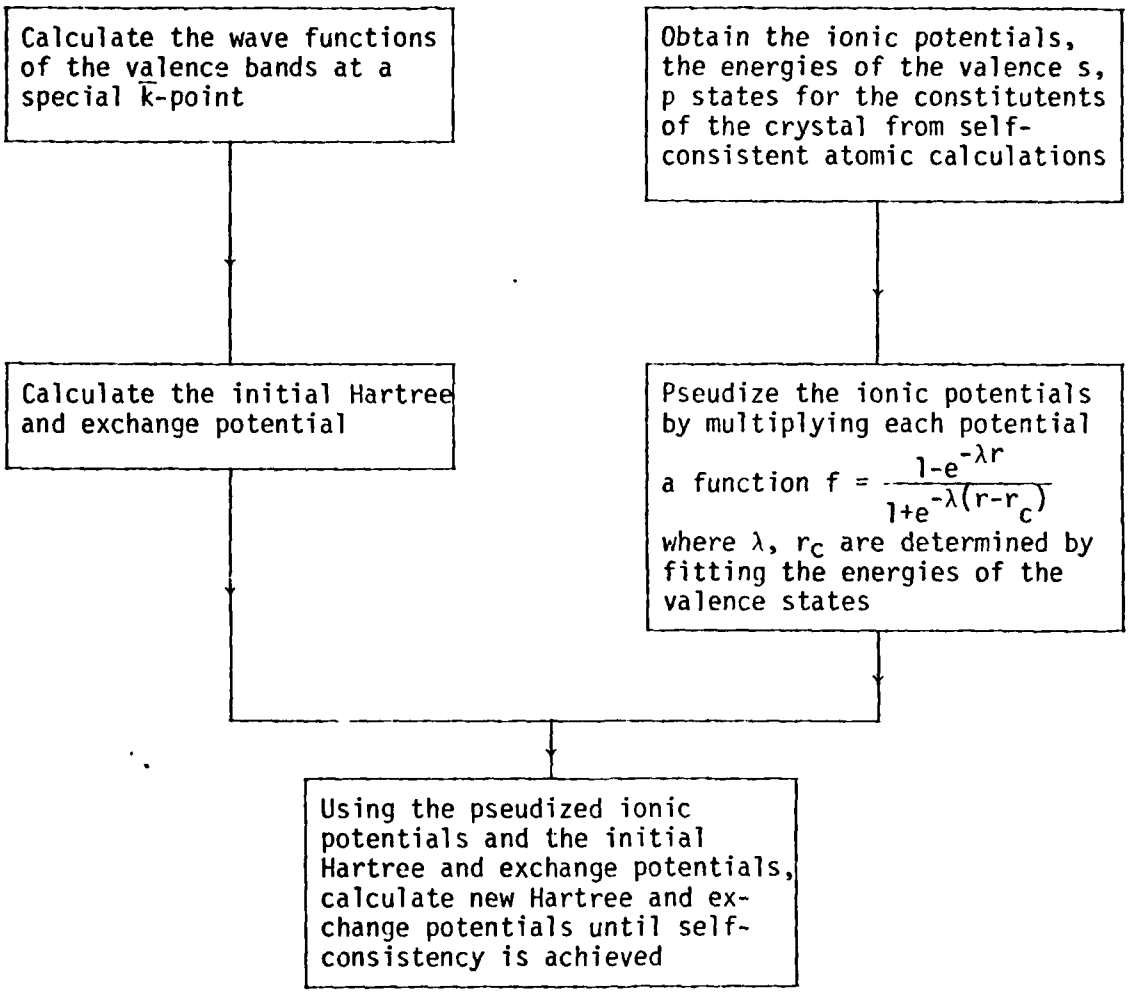
Calculate the wave functions of the valence bands at a special $\bar{k}$-point
Obtain the ionic potentials, the energies of the valence s, p states for the constitutents of the crystal from self-consistent atomic calculations
Calculate the initial Hartree and exchange potential
Pseudize the ionic potentials by multiplying each potential a function $f = \frac{1-e^{-\lambda r}}{1+e^{-\lambda(r-r_c)}}$ where λ, r_c are determined by fitting the energies of the valence states
Using the pseudized ionic potentials and the initial Hartree and exchange potentials, calculate new Hartree and exchange potentials until self-consistency is achieved

Figure 3

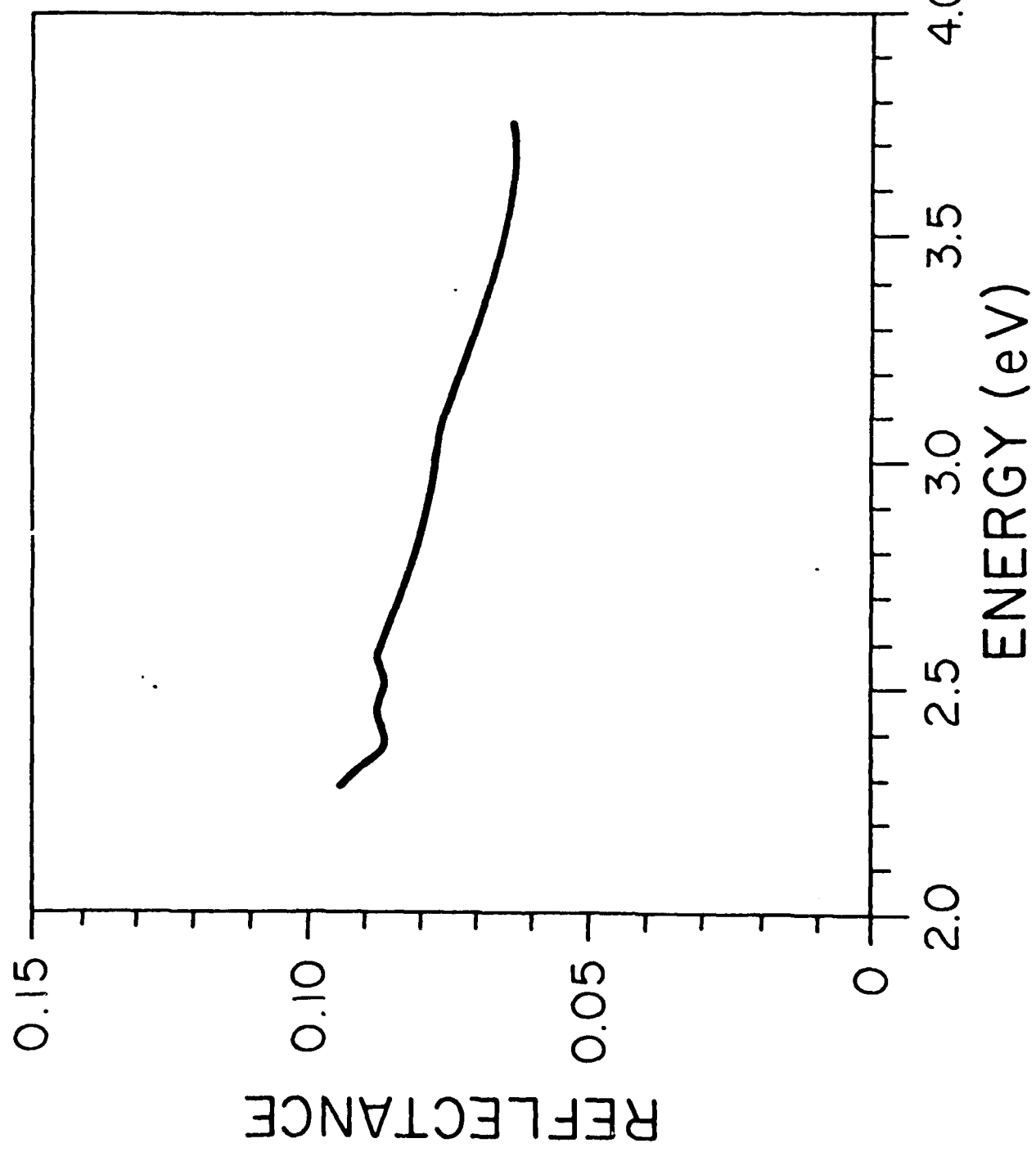

Figure 4

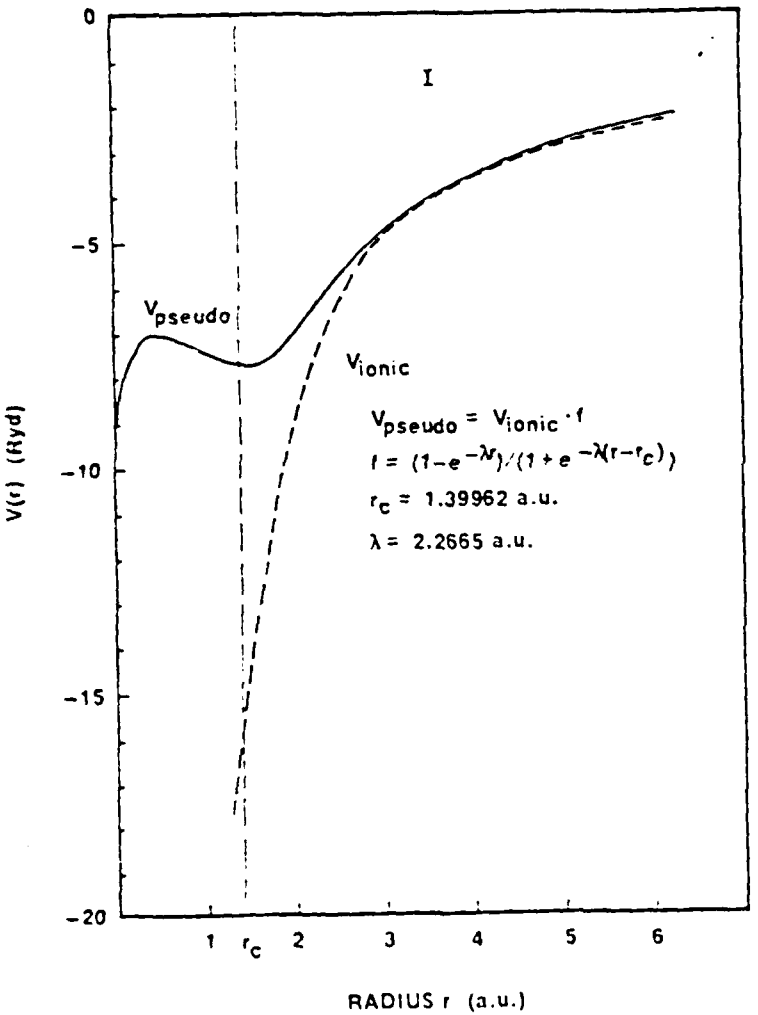

Figure 5a

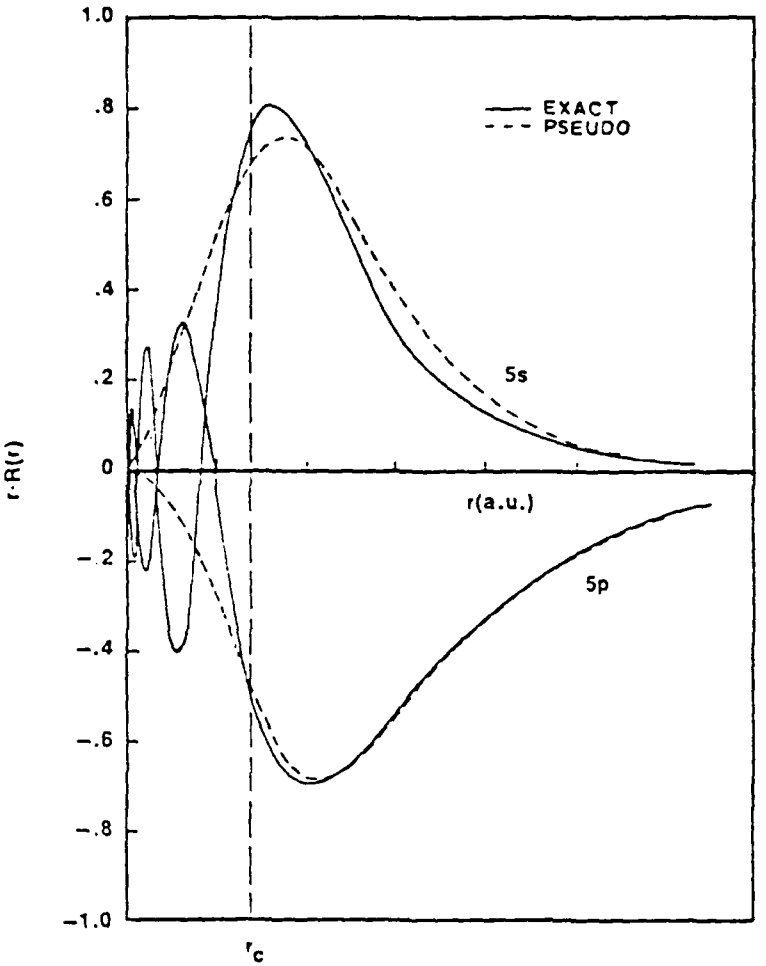

Figure 5b

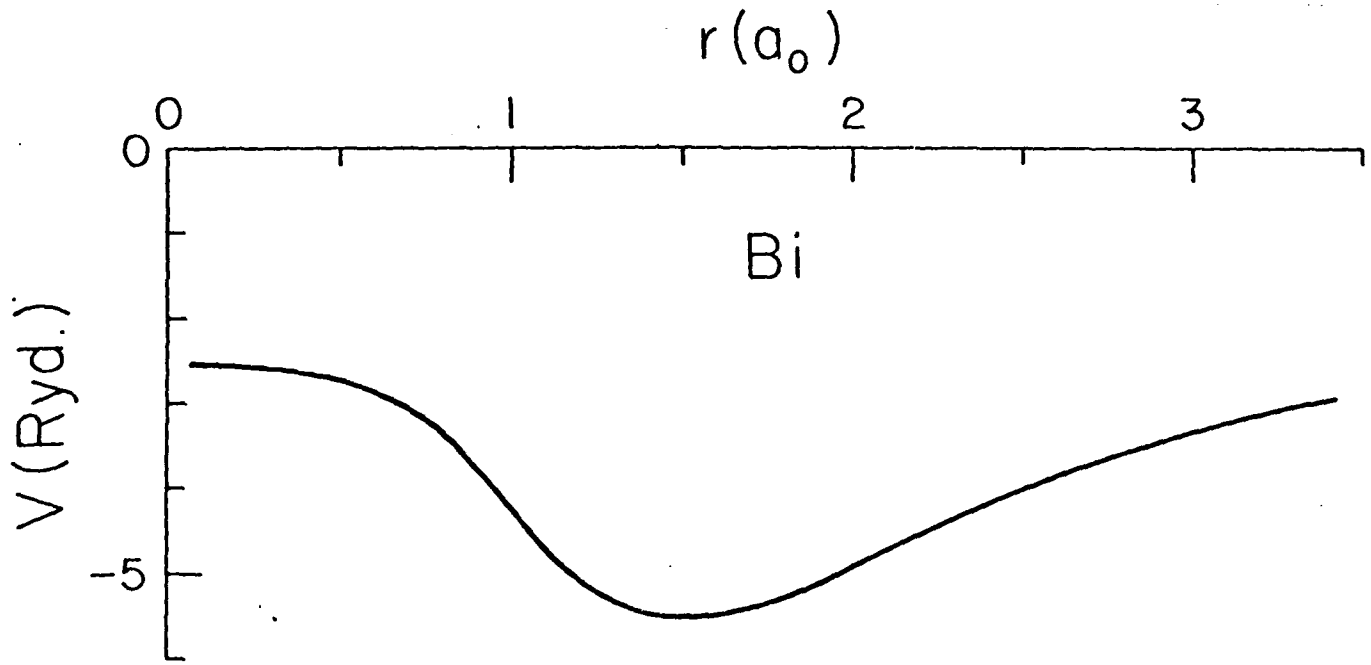

Figure 6a

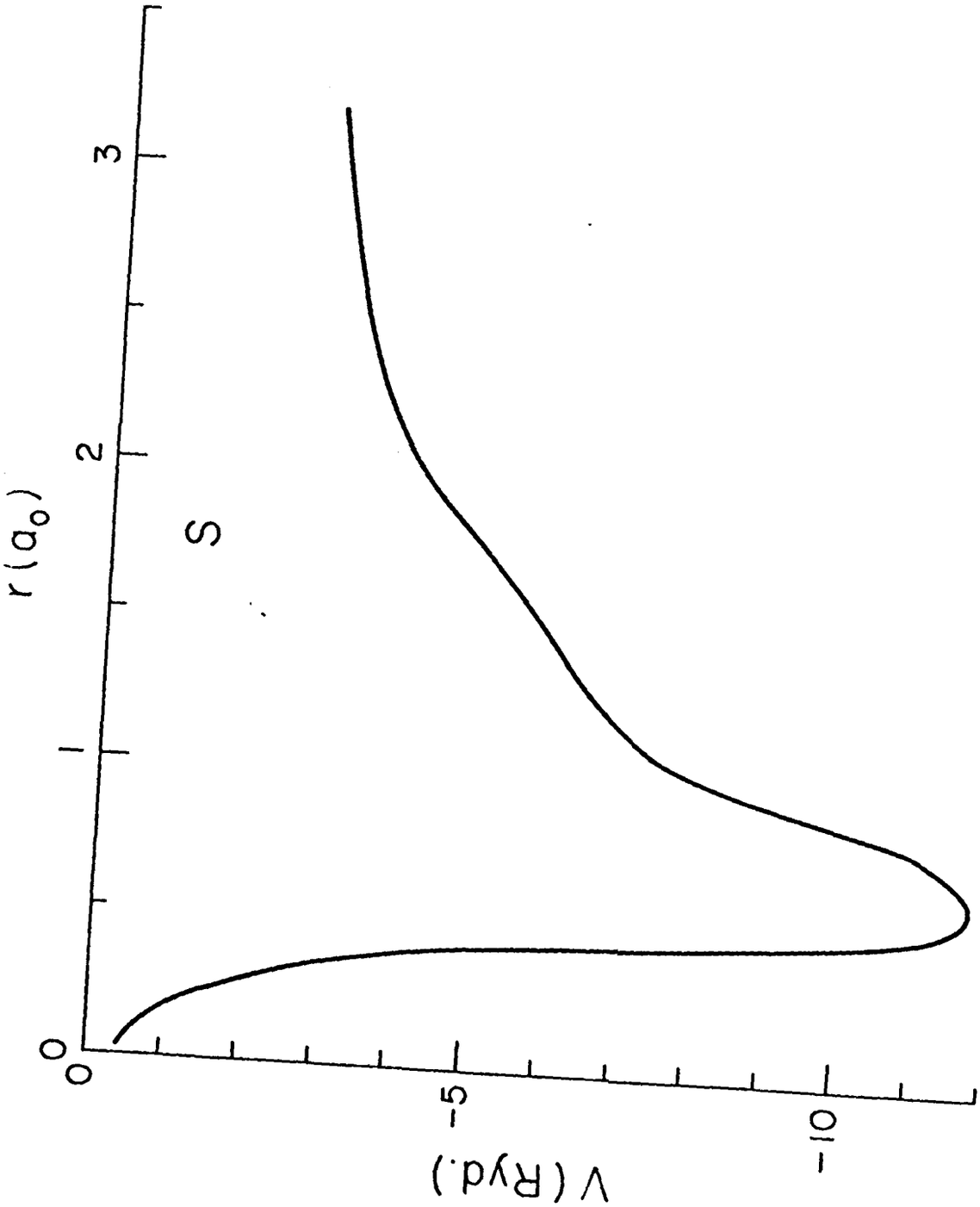

Figure 6b

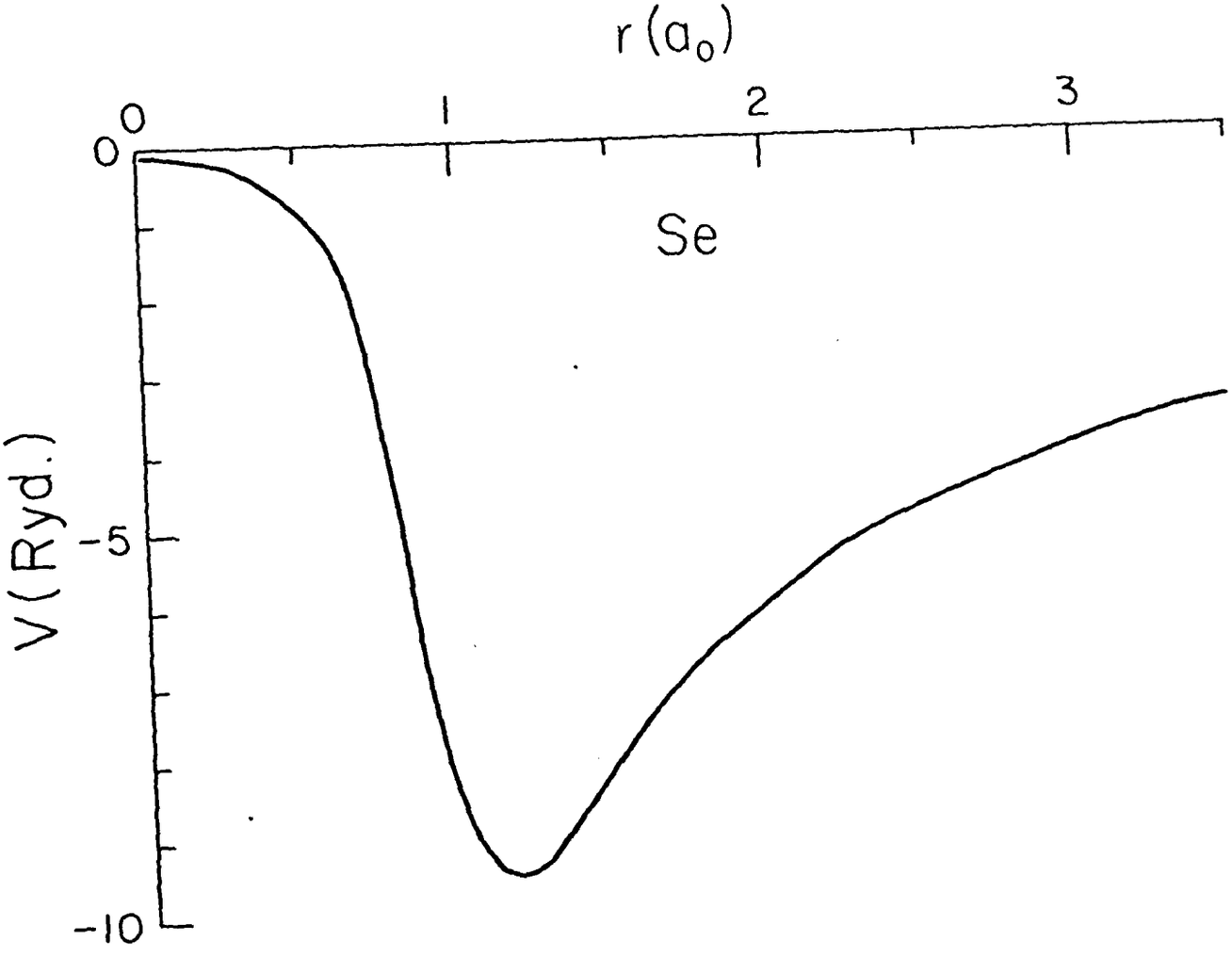

Figure 6c

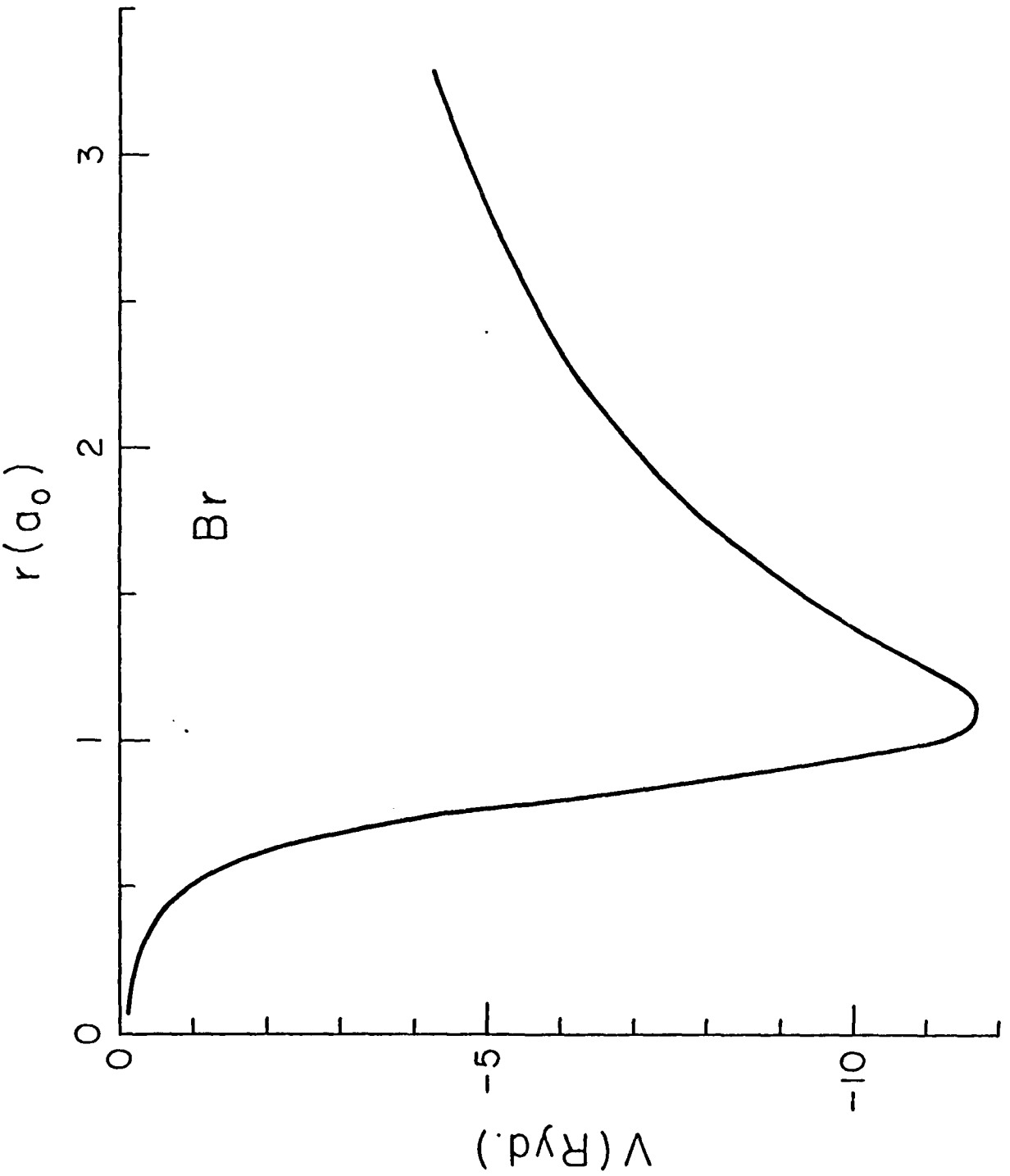

Figure 6d

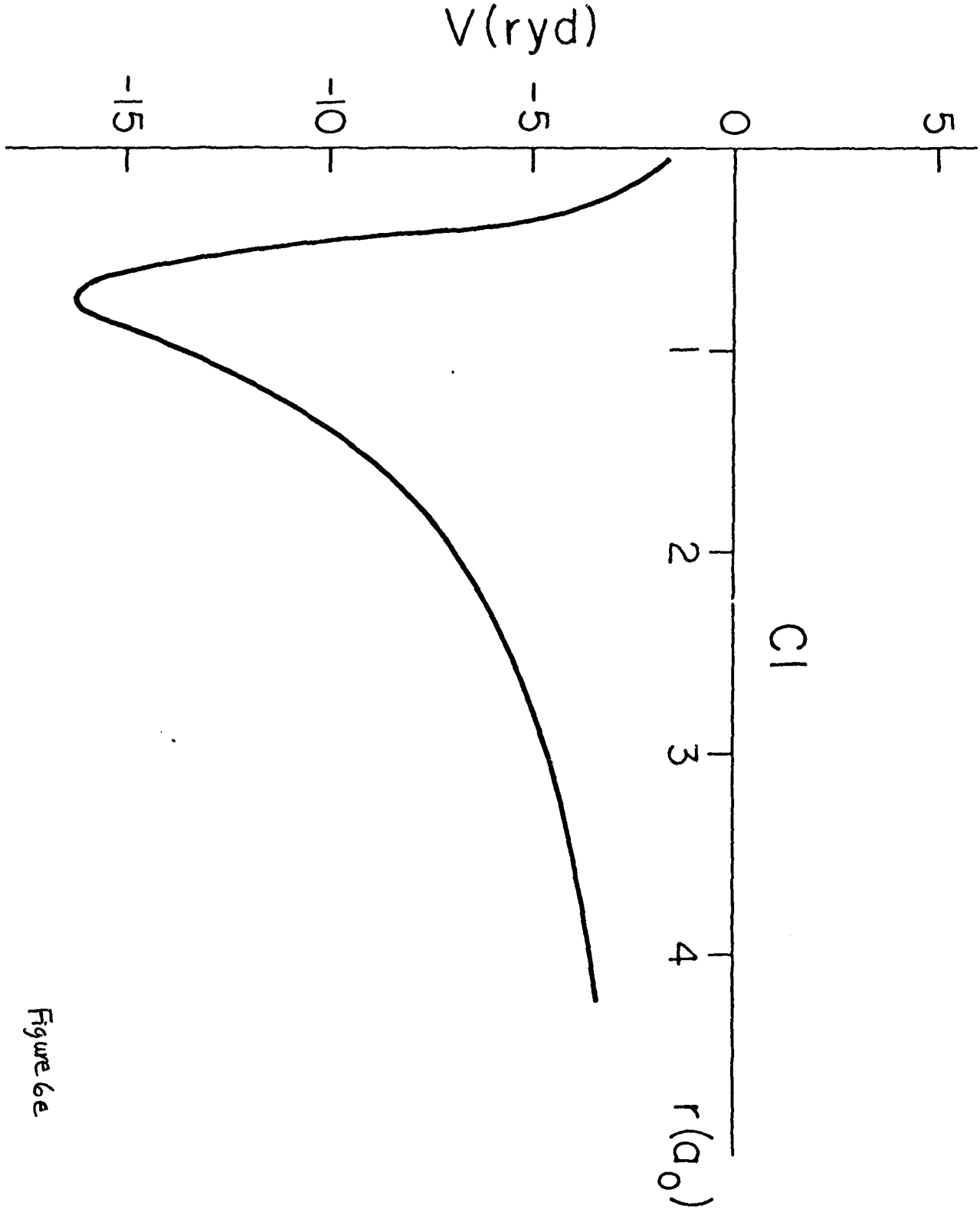

Figure 6e

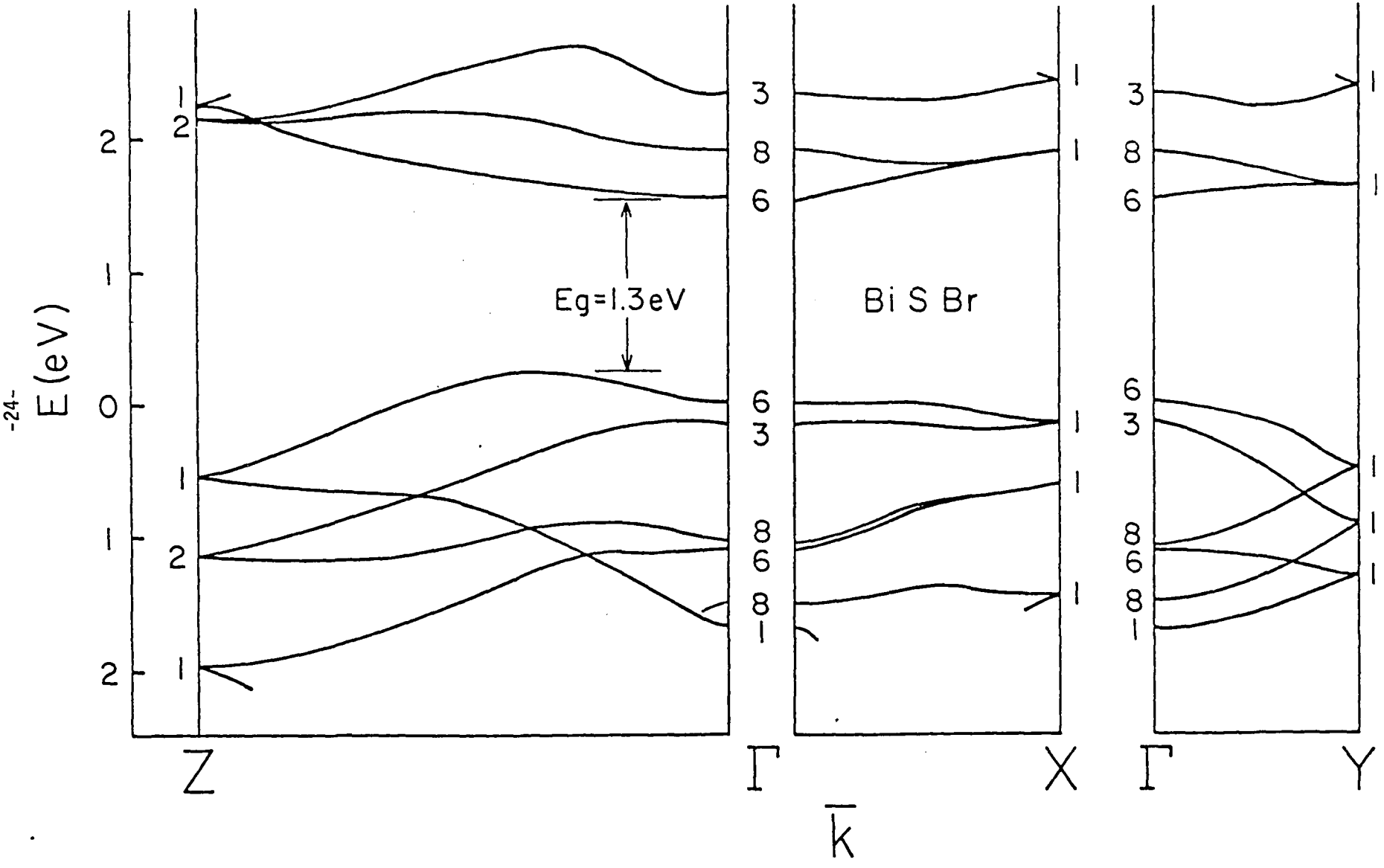

Figure 7a

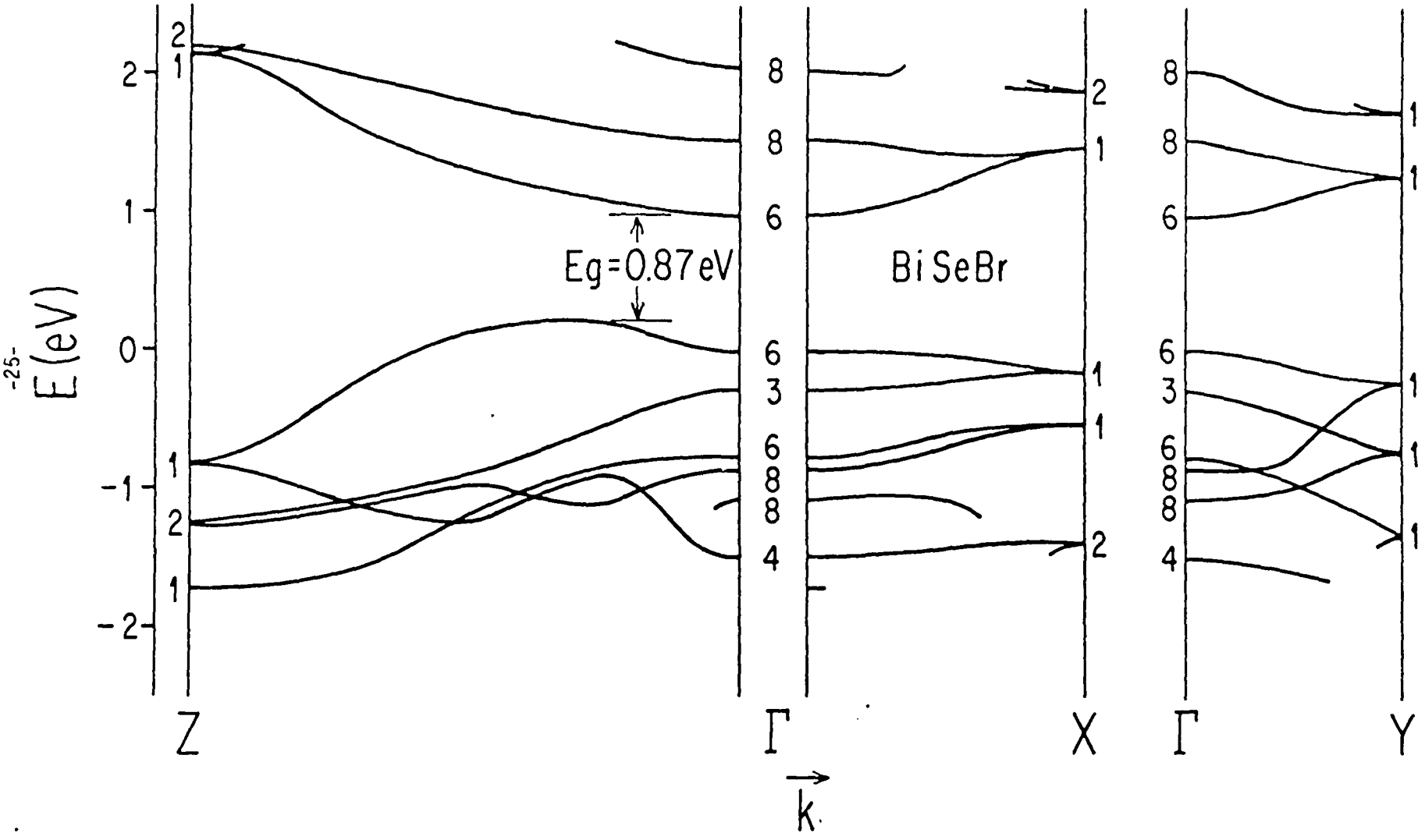

Figure 7b

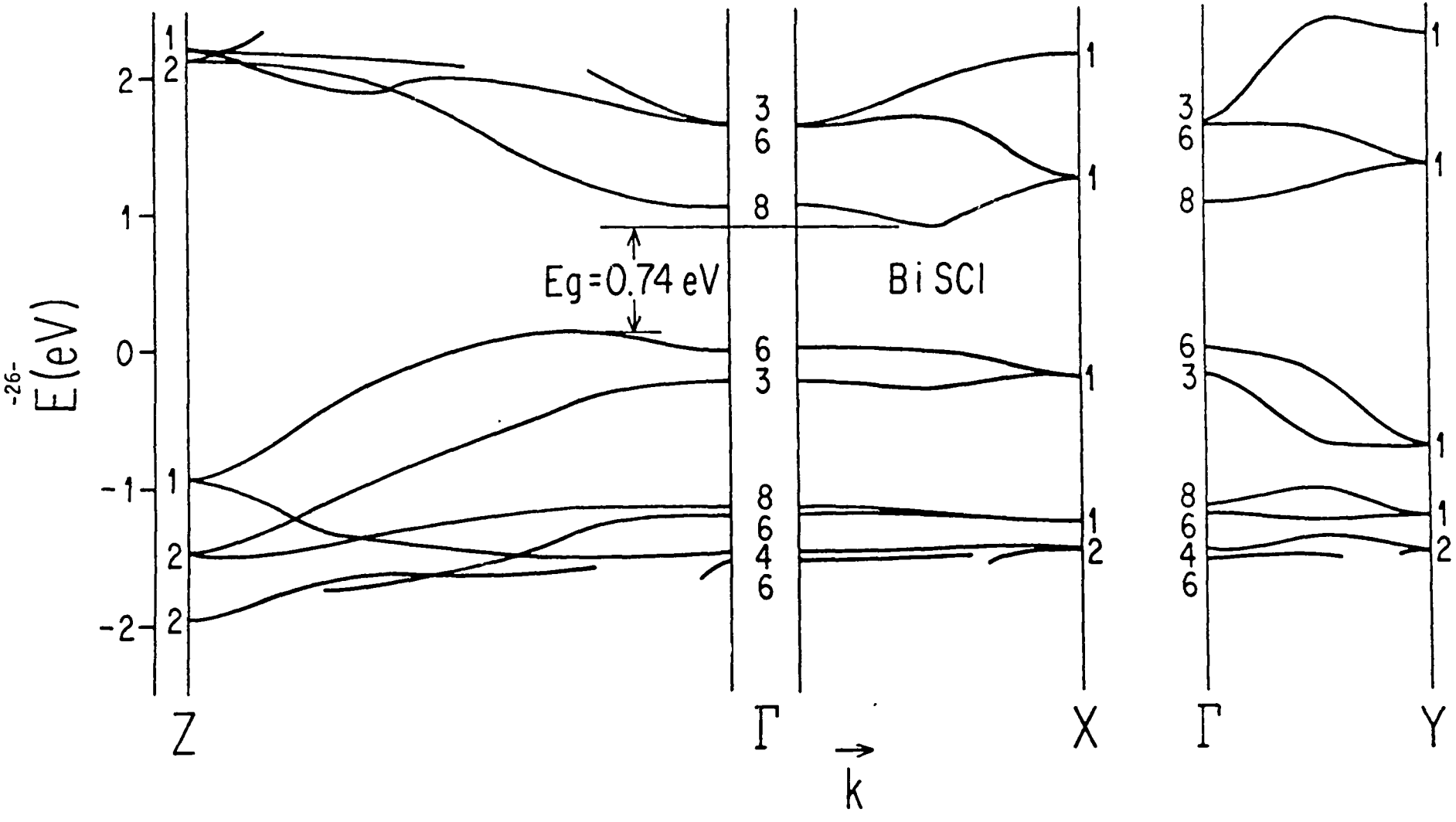

Figure 7c

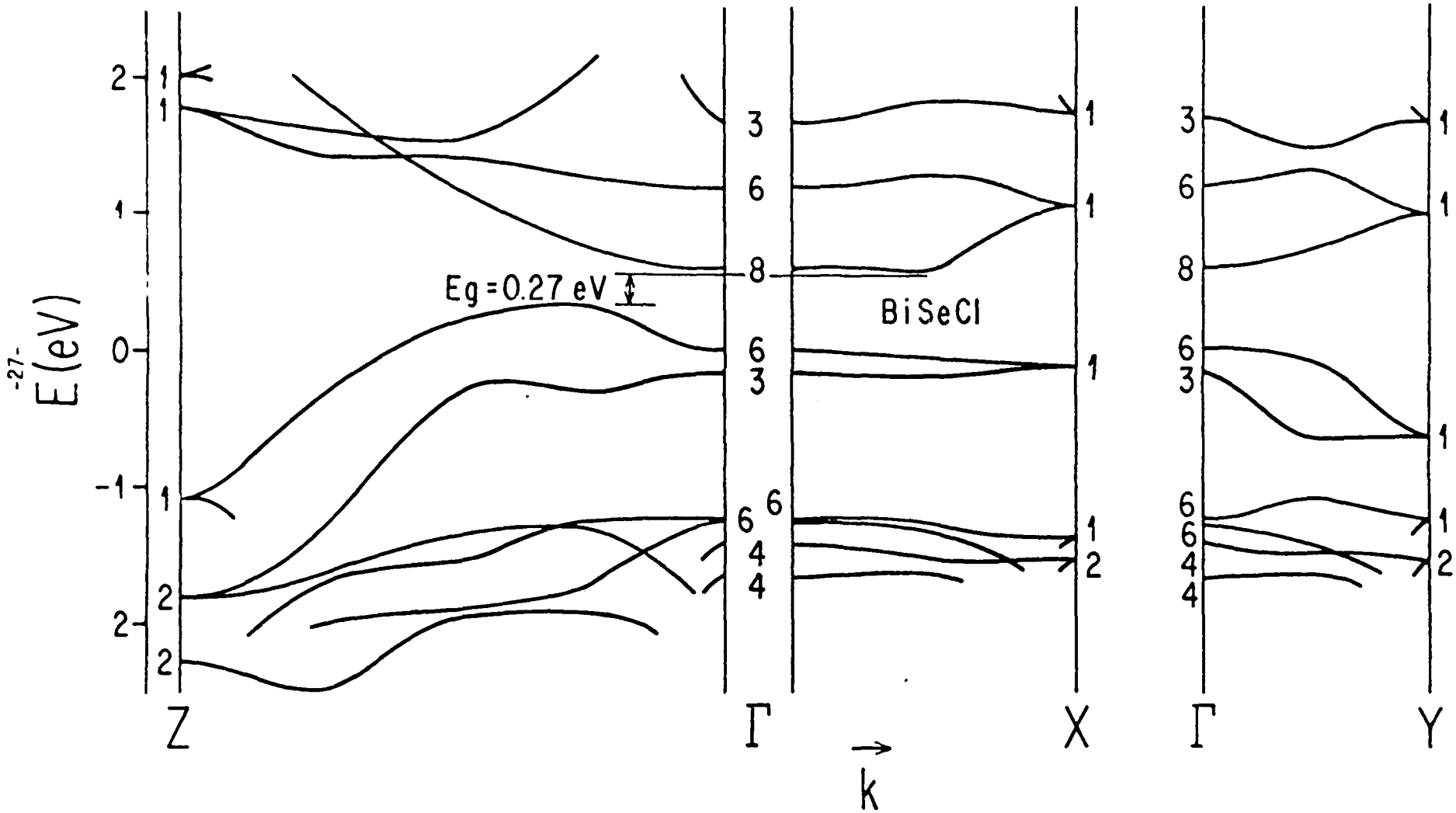

Figure 7d

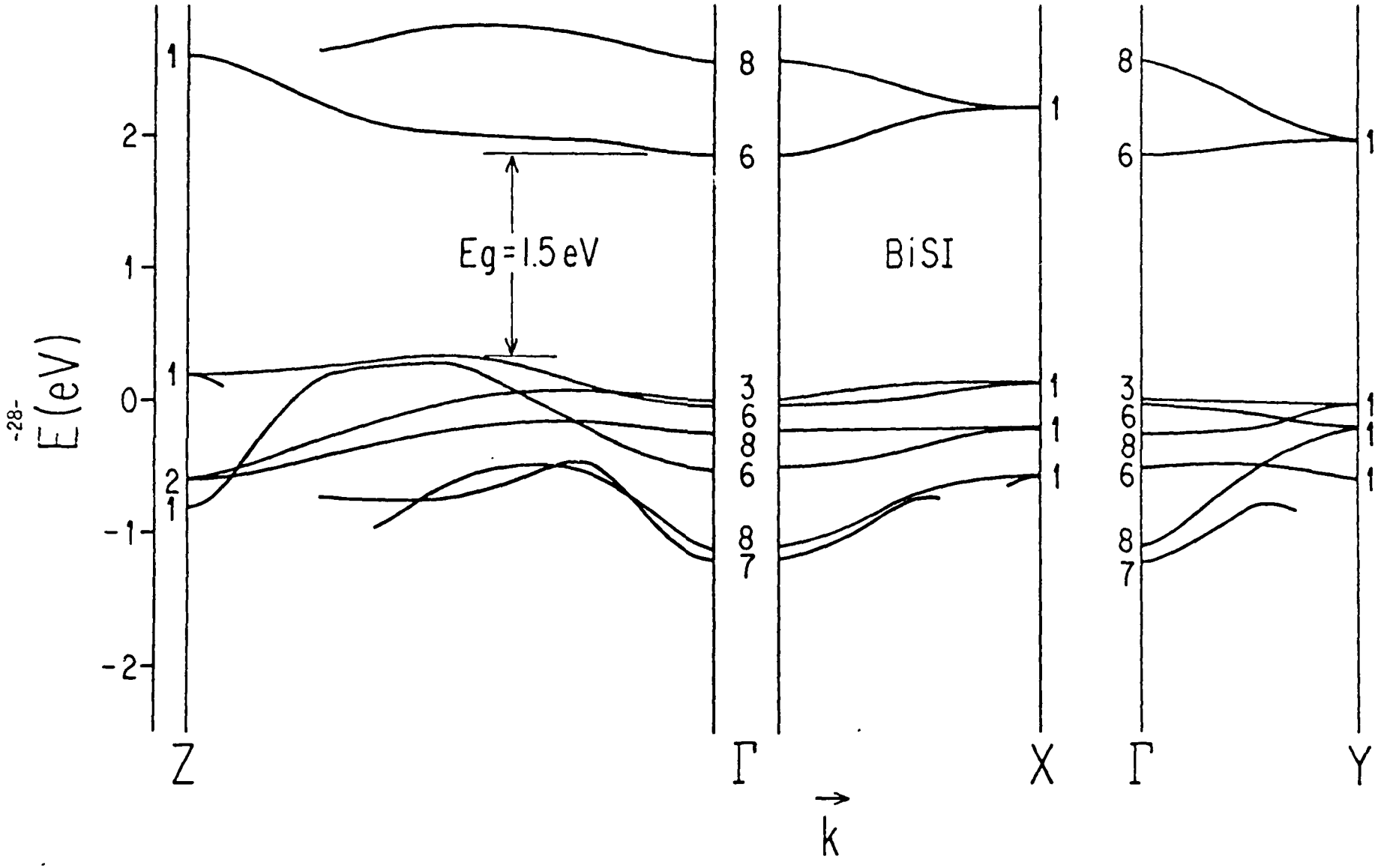
E(eV)
2
1
0
-1
-2
Eg=1.5 eV
BiSI
Z
Γ
X
Γ
Y
k
1
2
1
8
6
3
6
8
6
8
7
1
1
1
1
8
6
3
6
8
6
8
7
1
1
1
1

Figure 7e

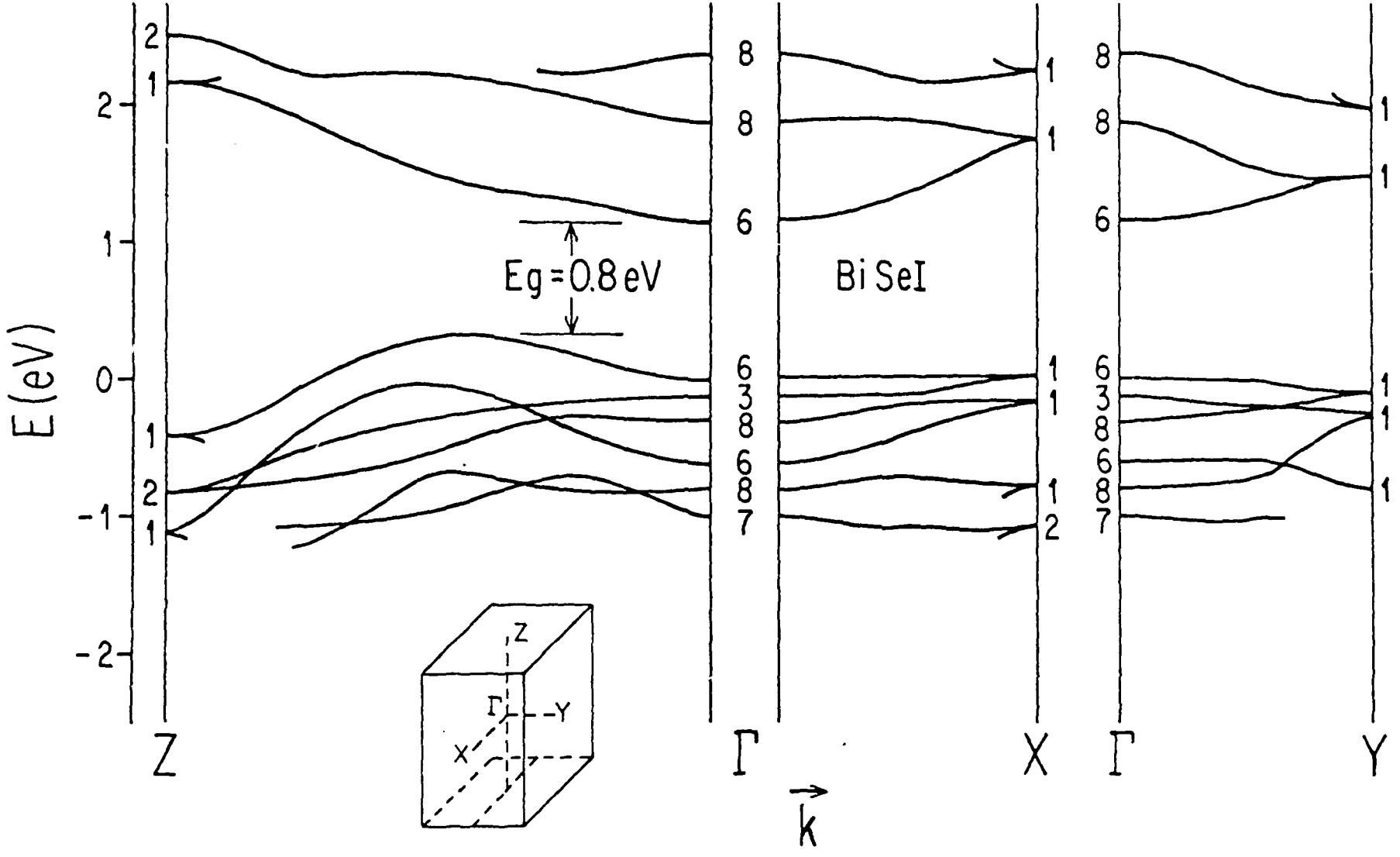

Figure 7f

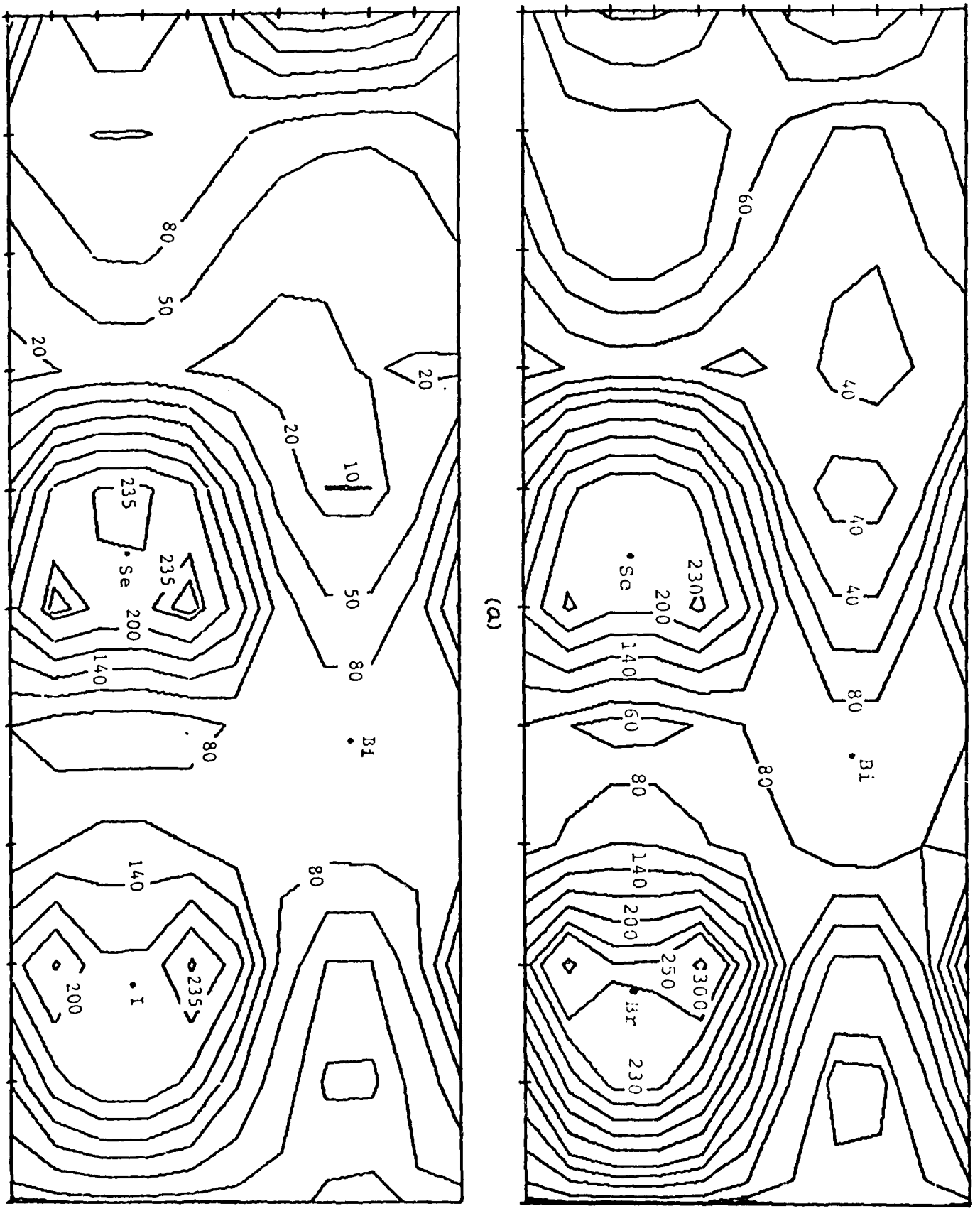

Figure 8

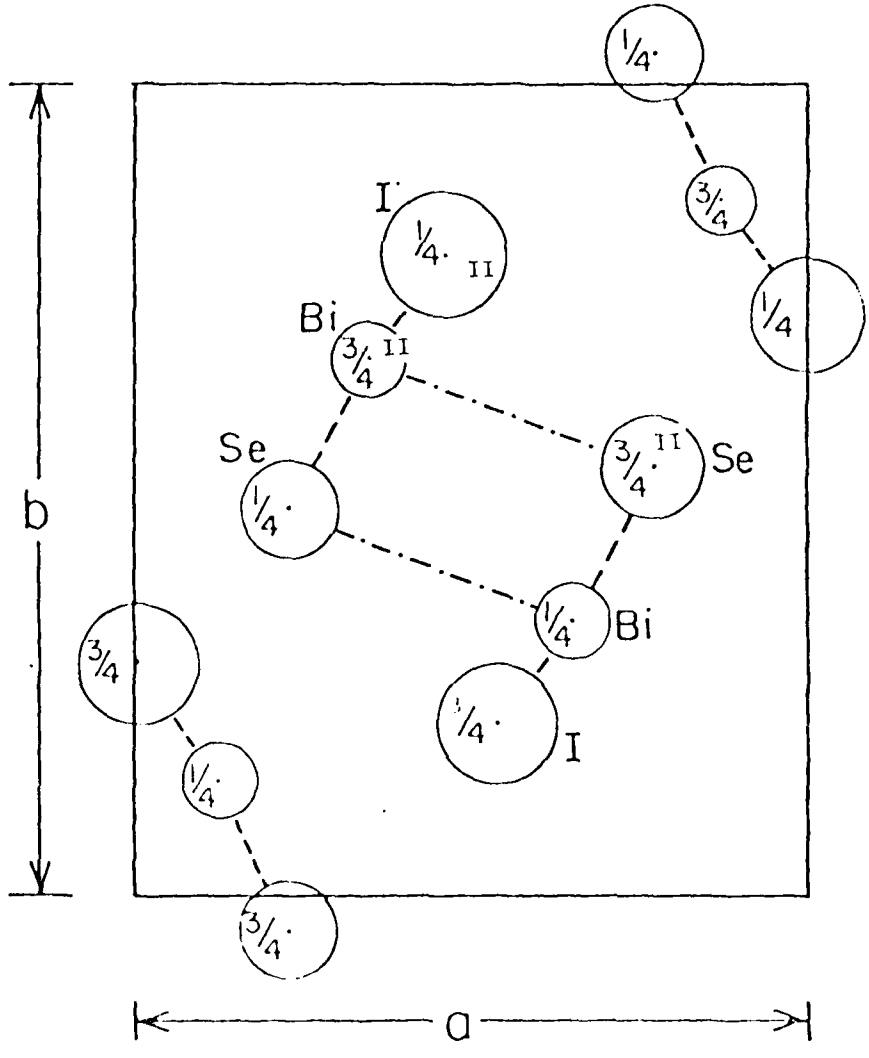

Figure 9

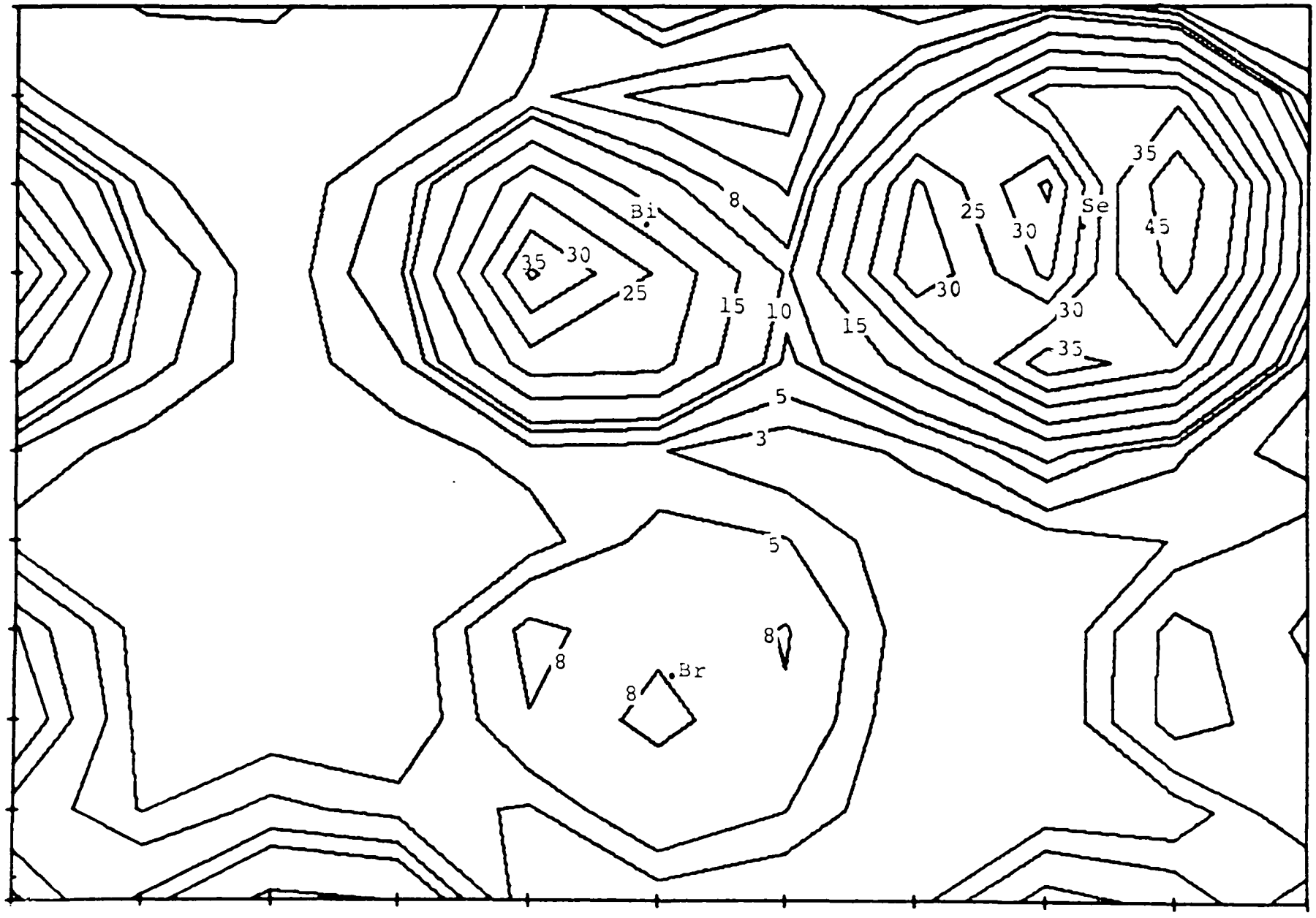

Figure 10a

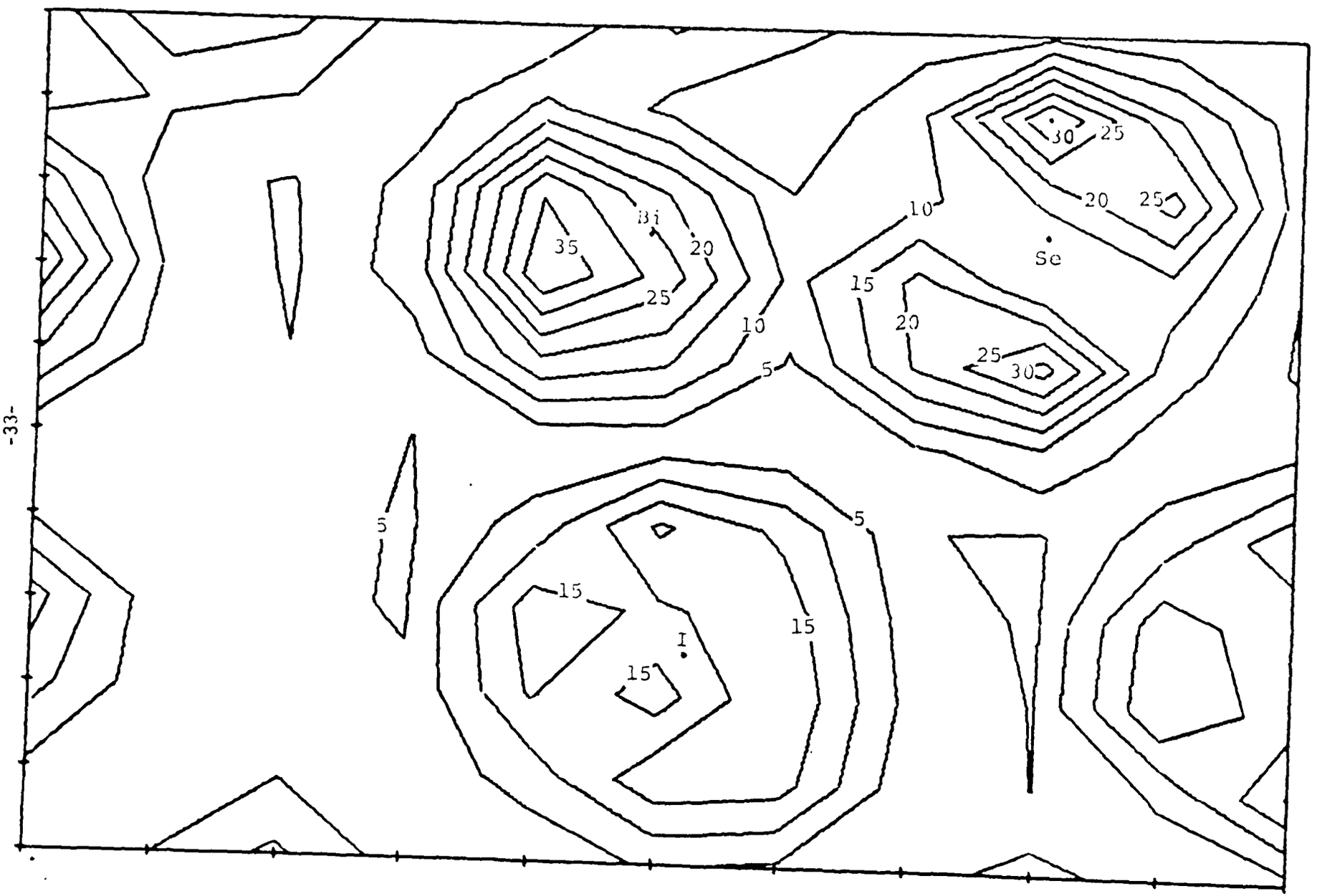

Figure 10b

Figure 11a

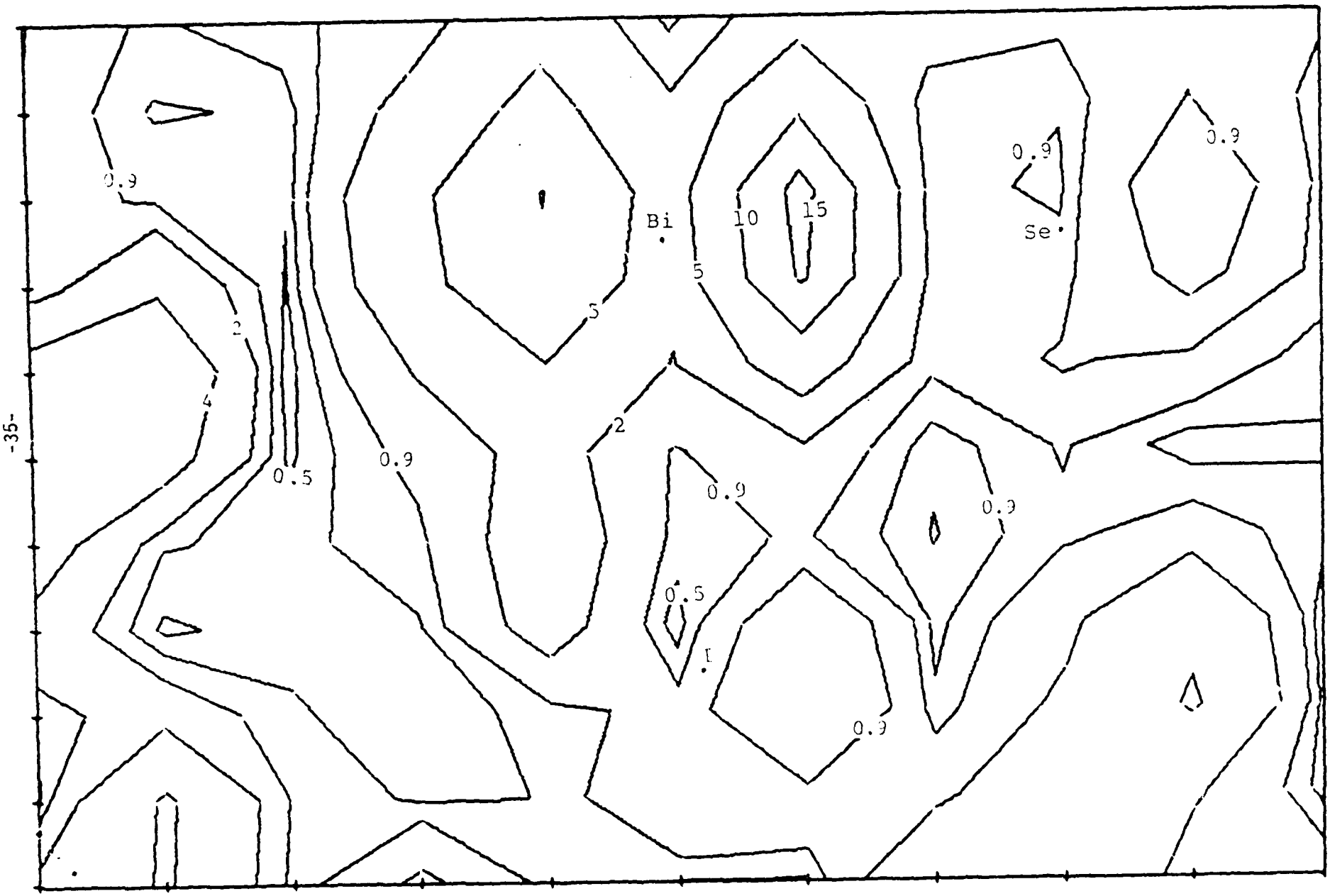

Figure 11 b

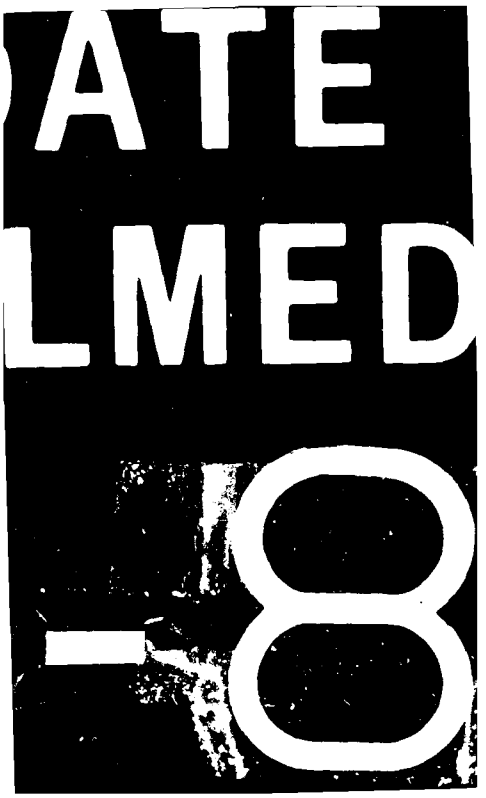
ATE
LMED
8